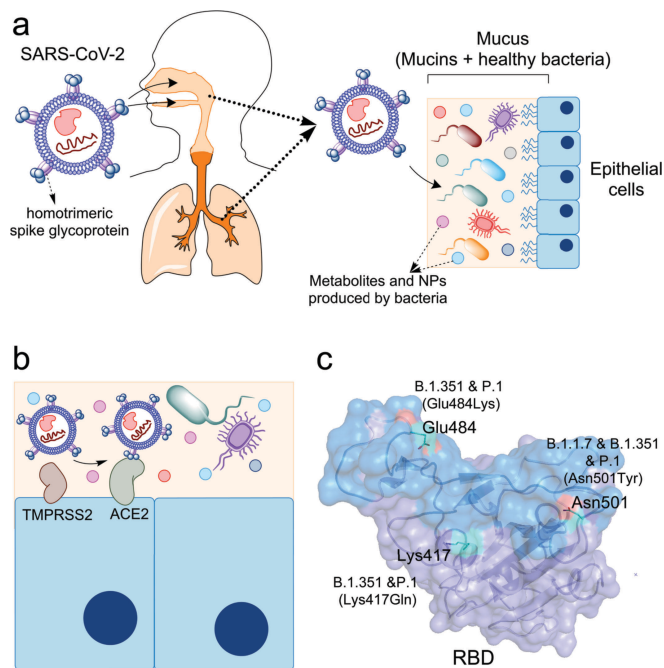


# Hidden in Plain Sight: Natural Products of Commensal Microbiota as an Environmental Selection Pressure for the Rise of New Variants of SARS-CoV-2

Jovan Dragelj,<sup>[a]</sup> Maria Andrea Mroginski,<sup>[a]</sup> and Kourosh H. Ebrahimi<sup>\*,[b]</sup>

Since the emergence of SARS-CoV-2, little attention has been paid to the interplay between the interaction of virus and commensal microbiota. Here, we used molecular docking and dynamics simulations to study the interaction of some of the known metabolites and natural products (NPs) produced by commensal microbiota with the receptor binding domain (RBD) of the spike glycoprotein of SARS-CoV-2. The results predict that NPs of commensal microbiota such as bile acids and non-ribosomal peptides (NRPs), of which some are siderophores, bind to the wild-type RBD and interfere with its binding to the ACE2 receptor. N501Y mutation, which is present in many of the emerging variants of the virus, abolishes the predicted binding pocket of bile acids and NRPs. Based on these findings, available experimental data showing that bile acids reduce the binding affinity of wild-type RBD to the ACE2 receptor, and the data suggesting that the respiratory tract microbiota affect viral infection we put forward the following proposal: mutations such as N501Y enable the RBD to bind to the ACE2 receptor more effectively in the presence of NPs produced by the respiratory tract bacteria thereby, increasing the infectivity rate of the virus. We hope our data stimulate future works to better understand the interactions of NPs produced by commensal microbiota with respiratory viruses like SARS-CoV-2.

Severe acute respiratory syndrome coronavirus 2 (SARS-CoV-2) has become a global emergency since early 2020. It is now clear that upon entry to the respiratory tract the virus uses its homotrimeric spike glycoprotein (S protein) to bind to its host-cell receptor angiotensin-converting enzyme 2 (ACE2) in the nasal epithelial cells,<sup>[1]</sup> the primary site of SARS-CoV-2 infection (Figure 1a). The respiratory tract is covered by mucus, which consists of mucins and various bacteria (Figure 1a).<sup>[2]</sup> This healthy mucus is the first barrier for respiratory viruses such as SARS-CoV-2. It is shown that bacteria residing in the respiratory



**Figure 1.** Mucus is the first barrier to the infection of epithelial cells by SARS-CoV-2. (a) SARS-CoV-2 is a respiratory virus and upon entry to the respiratory system of a healthy individual it faces mucus, which consists of mucin and a healthy population of bacteria. (b) After pathing through the mucus, viral entry to epithelial cells requires the proteolytic activity of TMPRSS2 to induce conformational changes in the spike glycoprotein. Consequently, RBD is exposed and interacts with the ACE2 receptor. (c) Structure of RBD (PDB Code: 7C8D). Mutations observed in the three major emerging variants of SARS-CoV-2 are shown (cyan). The Asn501Tyr (N501Y) mutation is seen among many variants. The surface of RBD that faces and interacts with the ACE2 receptor is colored in blue.

tract affect influenza virus infection.<sup>[3–5]</sup> The microbial community of the mucus is proposed to be the gatekeeper to respiratory health.<sup>[6]</sup> It is shown that changes in the population and diversity of these microbiota are linked to respiratory viral infections<sup>[3]</sup> including SARS-CoV-2.<sup>[7–9]</sup> *In-silico* studies predict that the upper respiratory tract (URT) bacteria produce proteins with the ability to bind to the RBD reducing its capacity to cause severe infection,<sup>[7]</sup> and more recently it is suggested that the virus may have phage-like behaviour.<sup>[10]</sup> In this respect, the potential interactions of natural products (NPs) of respiratory tract bacteria with SARS-CoV-2 has remained unexplored.

The primary site of the interaction of SARS-CoV-2 with the mucus and the host cell is its homotrimeric spike glycoprotein. For entry to the host cells, the spike glycoprotein interacts with

[a] Dr. J. Dragelj, Prof. M. A. Mroginski  
Institute of Chemistry,  
Technische Universität Berlin  
Straße des 17. Juni 135, 10623 Berlin (Germany)

[b] Dr. K. H. Ebrahimi  
Chemistry Research Laboratory  
Department of Chemistry, University of Oxford  
Mansfield Road, Oxford OX1 3TA (UK)  
E-mail: kourosh.honarmandebrahimi@chem.ox.ac.uk

Supporting information and the ORCID identification numbers for the authors of this article are available on the WWW under <https://doi.org/10.1002/cbic.202100346>.

the transmembrane protease, serine 2 (TMPRSS2) on the surface of target cells (Figure 1b). The proteolytic activity of TMPRSS2 induces a conformational change in the spike glycoprotein causing it to adopt an open state. Consequently, the receptor binding domain (RBD) of the spike glycoprotein is exposed and binds to the angiotensin-converting enzyme 2 (ACE2) allowing the virus to enter into the host cells (Figure 1b)<sup>[11]</sup> very similar to SARS-CoV-1.<sup>[12]</sup> In the case of SARS-CoV-2, neuropilin-1 (NRP1) is shown to be a host-cell factor helping viral entry and infection.<sup>[13]</sup> Emerging variants of the virus with higher mortality and infectivity rates are rapidly appearing around the globe. Some recent variants, which may resist antibody response,<sup>[14,15]</sup> include B.1.1.7 (the UK variant), B.1.351 (the South African variant), and P.1 (the Brazilian variant). All these variants have gained amino acid changes in the spike glycoprotein including mutations in the RBD (Figure 1c). The common mutation of the RBD among all these variants is the substitution of asparagine 501 by tyrosine (Asn501Tyr or N501Y) (Figure 1c). The emerging variants are shown to have a replicative advantage and higher transmissibility,<sup>[16,17]</sup> whose molecular mechanisms have remained vague. Molecular dynamics simulations suggest that the N501Y mutation may increase<sup>[18,19]</sup> or decrease<sup>[20]</sup> the binding affinity of RBD to the ACE2 receptor. On the other hand, studies using pseudotyped viruses revealed that N501Y mutation does not increase the infectivity rate of variants of SARS-CoV-2 as compared to the wild-type (WT) virus in cell-based assays.<sup>[21]</sup> More recent data using hamster models and cell-based assays show that the replication rates of the N501Y variants increase in the upper respiratory airway.<sup>[17]</sup> These contrasting findings suggested to us that additional factors in the respiratory tract might contribute to the difference between the lower infectivity rate of the wild-type virus and those of its emerging variants.

Because the first barrier for viral entry to host cells is mucus (Figure 1a), we hypothesized that metabolites or natural products (NPs) produced by bacteria residing in mucus can bind to the WT-RBD and interfere with its interaction with the ACE2 receptor and thus, viral entry to host cells. To test this hypothesis, we used molecular docking simulations taking advantage of the open source PyRx software (Supporting Methods),<sup>[22]</sup> which uses AutoDock Vina program.<sup>[23]</sup> We benchmarked our approach to estimate its accuracy. We predicted the binding pocket of a bisindolylmaleimide inhibitor into the catalytic domain of human protein kinase C (PKC)  $\beta$  II and compared the outcome with the reported structural data for the same inhibitor (Figure 2).<sup>[24]</sup>

The predicted binding pocket using PyRx software is identical to the observed binding pocket of the inhibitor in the X-ray crystal structure of PKC $\beta$ -II (Figure 2a). In both the predicted and the observed binding pockets the binding mode of the ligand is dictated by hydrophobic interactions (Figure 2b). The predicted Gibbs free energy ( $\Delta G$ ) of binding was  $-8.3$  (kCal/mol). Next, we aimed to estimate the error for the predicted  $\Delta G$ . We performed molecular docking simulations using four predicted ligands of RBD and compared our  $\Delta G$  values with those published using other molecular docking approaches (Supporting Methods). Using the predicted  $\Delta G$

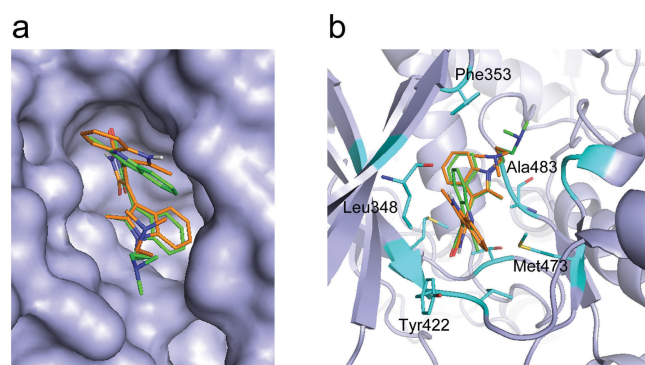


**Figure 2.** PyRx software reliably predicts binding pocket of ligands. (a) The predicted binding pocket of 2-methyl-1H-indol-3-yl-BIM-1 (ID: ZINC8431832) using PyRx software (orange) is identical to the observed binding pocket of this inhibitor (green) in the X-ray crystal structure of human PKC $\beta$ -II (PDB Code: 2I0E). (b) The binding mode and interactions predicted by PyRx software are similar to those observed in the X-ray crystal structure.

values obtain by our approach and those published previously, we estimated an error of  $\pm 0.55$  (kCal/mol). Thus, we used a  $\Delta G$  value of  $-8.3 \pm 0.55$  (kCal/mol) as a benchmark for identifying metabolites or NPs with a reasonable binding affinity to the RBD.

The current knowledge of the full spectrum of metabolites and NPs produced by respiratory tract bacteria is limited. Thus, we looked at some of the most common metabolites and NPs produced by commensal microbiota including amino acids, bile acids, non-ribosomal peptides (NRPs), and vitamins (Supporting Table S1).<sup>[25–27]</sup> We predicted the binding pocket of each metabolite and NP (Supporting Figures S1–S4) with the smallest Gibbs free energy ( $\Delta G$ ), which we used to estimate the dissociation constants ( $K_d$ ) (Supporting Methods). Among various molecules tested, tauro- $\alpha$ -muricholic acid, taurocholic acid, enterobactin, and tilivalline have a  $\Delta G$  value close to the benchmarked value of  $-8.3 \pm 0.55$  (kCal/ml). Thus, these molecules have a reasonable binding affinity with calculated  $K_d$  values of 0.45, 1.00, 0.74 and 0.82 mM, respectively (Supporting Table S1). These values are less than that of folic acid (vitamin B9) ( $K_d = 2.1$  mM), which is predicted to bind to the RBD<sup>[28]</sup> and might help in treating COVID-19 patients.<sup>[29,30]</sup> As an example, the predicted binding pockets for tauro- $\alpha$ -muricholic acid (Figure 3a) and tilivalline (Figure 3b) are shown. The binding mode of tauro- $\alpha$ -muricholic acid and tilivalline includes hydrogen bonds and hydrophobic interactions (Supporting Figure S5). Tauro-alpha-muricholic acid, taurocholic acid, enterobactin and tilivalline have some common features: they all have aromatic and aromatic hydroxyl groups. These functional groups are present in other ligands like terpenes and drugs, which are predicted to bind to the same binding pocket in the RBD.<sup>[31,32]</sup> Additionally, these functional groups are present in other bile acids<sup>[33]</sup> and the drug Corilagin,<sup>[34]</sup> which are shown to interfere with the RBD binding to the ACE2 receptor in biochemical assays. The predicted binding pocket for NPs like bile acids and NRPs includes Asn501 (N501) (Figures 3a–b and Supporting Figures S1–S4). Alignment of the predicted binding

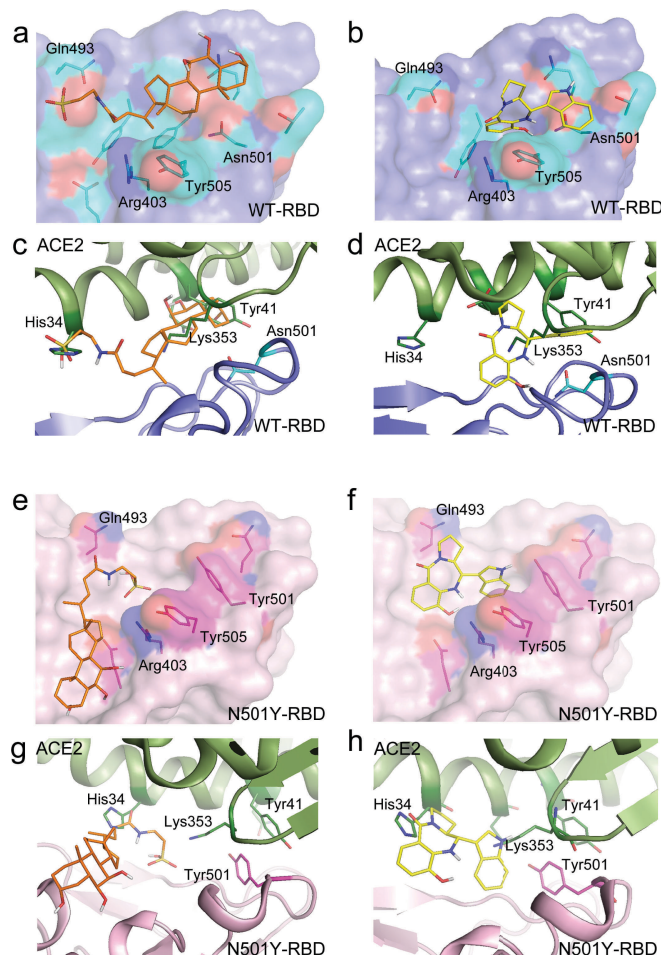


**Figure 3.** Asn501Tyr (N501Y) mutation abolishes the binding pocket of bile acids and NRPs in the WT-RBD. (a) The predicted binding site of tauro- $\alpha$ -muricholic acid (orange) and (b) that of tilivalline (yellow) in WT-RBD. In this binding site (c) tauro- $\alpha$ -muricholic acid and (d) tilivalline interfere with the WT-RBD binding to the ACE2 receptor as observed by aligning the predicted binding sites with the solved structure of RBD-ACE2 receptor (PDB Code: 7C8D). (e) Asn501Tyr (N501Y) mutation shifts the binding pocket of tauro- $\alpha$ -muricholic acid (orange) and (f) tilivalline (yellow). The new binding pocket has a significantly lower affinity for these NPs (Supporting Table S1) and in this pocket the interference of (g) tauro- $\alpha$ -muricholic acid (orange) and (h) tilivalline with the N501Y-RBD binding to the ACE2 receptor is minimized as observed by aligning the predicted binding site with the solved structure of RBD-ACE2 receptor (PDB Code: 7NXC).

pocket with the structure of RBD-ACE2 complex revealed that bile acids like tauro- $\alpha$ -muricholic acid (Figure 3c) and NRPs like tilivalline (Figure 3d) directly interfere with the interactions between the amino acid residues of WT-RBD and those of the ACE2 receptor. These data strongly suggest that NPs produced by commensal microbiota interfere with the WT-RBD binding to the ACE2 receptor consistent with the reported biochemical data for bile acids.<sup>[33]</sup> Since the predicted binding pocket for most of the NPs includes the amino acid Asn501 (Figures 3a–b and Supporting Figures S1–S4), which in many of the emerging variants of SARS-CoV-2 is replaced by a tyrosine (N501Y) (Figure 1c), we hypothesized that this mutation could interfere with the binding of bile acids and NRPs to the RBD. Therefore, we tested the binding of metabolites and NPs (Supporting

Table S1) to the RBD of a variant harboring N501Y mutation (N501Y-RBD). Molecular docking studies revealed that N501Y mutation abolishes the binding pocket of bile acids and NRPs observed in the WT-RBD (Supporting Table S1 and Figures 3e–f). In the case of tauro- $\alpha$ -muricholic acid and tilivalline, the predicted  $K_d$  values are 2.22 and 2.45 mM, respectively. These values within the estimated error are significantly larger (about 5-fold) than those of tauro- $\alpha$ -muricholic acid and tilivalline binding to the WT-RBD. Additionally, in the N501Y-RBD the predicted binding pocket of tauro- $\alpha$ -muricholic acid (Figure 3g), tilivalline (Figure 3h), and other bile acids and NRPs (Supporting Figures S6–S9) shifted. In this new binding pocket, the interference of NPs with the binding of N501Y-RBD to the ACE2 receptor is minimized (Figures 3g–h). The reason for the shift in binding site is potentially the bulky phenol group of Tyr501.

The predicted binding pocket of bile acids and NRPs does not have a glycosylation site; however, there is a distal glycosylation site (N343) (Supporting Figure S10).<sup>[35]</sup> The N343 glycans are important for the flexibility of the RBD during its exposure but not its direct interaction with the ACE2 receptor.<sup>[36,37]</sup> Consistently, using molecular docking studies we did not observe a difference between the binding pocket of NPs like taurocholic acid and tilivalline in the glycosylated RBD (N343) as compared with the not-glycosylated RBD (Supporting Figure S10). To further evaluate the results of molecular docking studies, we performed classical all atoms molecular dynamics (MD) simulations of glycosylated structures of WT-RBD and of the N501Y-RBD, both in complex with tilivalline. We first used MD simulations to evaluate the flexibility of tyrosine in the presence of tilivalline as a ligand. In our MD simulations, tyrosine did not show significant flexibility (Supporting Figure S11) supporting the proposal that its bulky phenol group interferes with the binding of bile acids and NRPs to the RBD. Next, we used MD simulations to study the conformational stability of tilivalline in the predicted binding site of glycosylated structures of WT-RBD and N501Y-RBD. The interaction energy between tilivalline and the RBD binding site averaged over the last 4 ns of the MDs simulations (Supporting Figure S12), was predicted to be as low as  $-10.26$  kcal/mol for the N501Y-RBD and below  $-17.08$  kcal/mol for the WT-RBD. When bound to the N501Y-RBD, tilivalline mostly interacts with the amino acid residues of RBD (Y501 and Y505) in such a way that it is positioned at the edge of the interface with the ACE2 receptor as revealed by close inspection of the MD trajectories (Supporting Figure S13). This observation suggests that tilivalline will be easily displaced by the N501Y-RBD binding to the ACE2 receptor. Therefore, we conclude that MD simulations reproduce the trend predicted by a static docking approach: i.e. N501Y mutation interferes with the binding of bile acids and NRPs to the RBD.

In summary, our *in-silico* studies revealed that NPs of commensal microbiota like bile acids and NRPs can bind to the WT-RBD of SARS-CoV-2 with a reasonable affinity and that N501Y mutation interferes with their binding to the RBD. Although we could not obtain experimental data in support of our *in-silico* studies, earlier biochemical studies have reported that bile acids interfere with the interaction of WT-RBD with the

ACE2 receptor.<sup>[33]</sup> Additionally, our knowledge of NPs produced by the respiratory tract microbiota is very limited and it is likely that they produce unknown NPs with higher binding affinity to the RBD. Hence, we postulate that NPs produced by the commensal microbiota, e.g. bile acids or NRPs, interact with the WT-RBD and these interactions reduce the binding affinity (or increase the  $K_d$ ) of the spike glycoprotein of SARS-CoV-2 to the ACE2 receptor. In the emerging variants with mutations such as N501Y, bile acids or NRPs cannot effectively interact with the RBD and thus, do not interfere with viral entry to host cells. Alternatively, it is possible that N501Y or other mutations of the RBD like those present in the B.1.617.2 variant (delta variant, which was first detected in India) increase the interactions of RBD with the ACE2 receptor<sup>[38]</sup> and thus, improving its binding to the ACE2 receptor in the presence of microbial NPs (Figure 4a).

This proposal helps in understanding the molecular mechanism underlying the emergence and the higher infectivity rates of new variants of SARS-CoV-2. Accordingly, we put forward a hypothetical model for a role of the respiratory tract bacteria in the evolution of SARS-CoV-2 (Figure 4b). The selection pressure induced by the host continuously directs the evolution and

adaptation of the virus. For the spike glycoprotein variants of SARS-CoV-2 at least two environmental selection pressures exist: the antibodies produced by the immune system and the healthy bacteria in the mucus, which is the first barrier for viral entry to the host cells. Future studies are needed to test the validity of this hypothesis. Moreover, our findings suggest that a change in the population of the healthy bacteria of the respiratory tract, which may occur due to ageing and smoking,<sup>[39,40]</sup> could contribute to the severity of the disease consistent with previous reports.<sup>[7–9]</sup> Our in-silico studies suggest that NPs produced by commensal microbiota may have therapeutic applications. We hope our findings stimulate future works to study and discover NPs produced by various bacteria living in the respiratory tract and to better understand their interactions with respiratory viruses like SARS-CoV-2.

## Acknowledgements

K.H.E. thanks Professor Fraser A. Armstrong (University of Oxford) and Professor Wilfred R. Hagen (TU Delft), Professor William James (University of Oxford) and Professor James McCullagh (University of Oxford) for their generous support. K.H.E. is grateful to the European Molecular Biology Organization (EMBO) (EMBO ALTF 157-2015), COST (European Cooperation in Science and Technology) Action CA15133 (ECOST-STSM-Request-CA15133-44200), and CRUK Oxford Developmental Fund (CRUKDF-0221-KHE) for generous financial support of his research. M.A.M. and J.D. acknowledge funding by the Deutsche Forschungsgemeinschaft (DFG, German Research Foundation) under Germany's Excellence Strategy – EXC 2008-390540038-UniSysCat.

## Conflict of Interest

The authors declare no conflict of interest.

**Keywords:** bile acids · commensal microbiota · natural products · NRPs · SARS-CoV-2

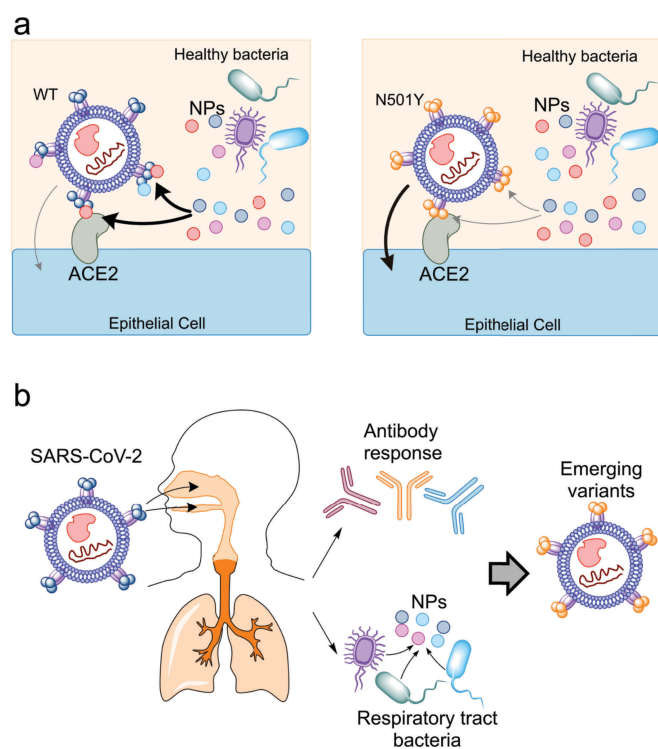


**Figure 4.** NPs produced by healthy bacteria in mucus are an environmental selection pressure for the rise of variants of respiratory viruses like SARS-CoV-2. (a) NPs like bile acids and/or NRPs produced by healthy bacteria interfere with the WT-RBD binding to the ACE2 receptor. The N501Y mutation or other mutations interfere with the binding of NPs with the RBD and/or increase the interaction of RBD with the ACE2 receptor. Consequently, they enable the virus to scape NPs of healthy bacteria and thus, they increase the infectivity of the virus. (b) Upon viral entry to the human body, the spike glycoprotein of the virus interacts with NPs produced by bacteria in the mucus. These NPs act as an environmental selection pressure together with antibody response leading to the emergence of new variants of SARS-CoV-2 with higher infectivity and/or mortality rates.

- [1] W. Sungnak, N. Huang, C. Becavin, M. Berg, R. Queen, M. Litvinukova, C. Talavera-Lopez, H. Maatz, D. Reichart, F. Sampaziotis, K. B. Worlock, M. Yoshida, J. L. Barnes, H. L. B. Network, *Nat. Med.* **2020**, *26*, 681–687.
- [2] B. X. Wang, C. M. Wu, K. Ribbeck, *FEBS J.* **2020**, *288*, 1789–1799.
- [3] M. Hauptmann, U. E. Schaible, *FEBS Lett.* **2016**, *590*, 3721–3738.
- [4] U. Neu, B. A. Mainou, *PLoS Pathog.* **2020**, *16*, e1008234.
- [5] N. Li, W.-T. Ma, M. Pang, Q.-L. Fan, J.-L. Hua, *Front. Immunol.* **2019**, *10*, 1551.
- [6] W. H. Man, W. A. A. de Steenhuisen, D. Bogaert, *Nat. Rev. Microbiol.* **2017**, *15*, 259–270.
- [7] K. H. Ebrahimi, *FEBS Lett.* **2020**, *594*, 1651–1660.
- [8] K. Kalantar-Zadeh, S. A. Ward, K. Kalantar-Zadeh, E. M. El-Omar, *ACS Nanotechnol.* **2020**, *14*, 5179–5182.
- [9] Y. He, J. Wang, F. Li, Y. Shi, *Front. Microbiol.* **2020**, *11*, 1302.
- [10] M. Petrillo, C. Brogna, S. Cristoni, M. Querci, O. Piazza, G. Van den Eede, *F1000Research* **2021**, *10*, 370.
- [11] A. C. Walls, Y.-J. Park, M. A. Tortorici, A. Wall, A. T. McGuire, D. Veelsler, *Cell* **2020**, *181*, 281–292.

- [12] W. Li, M. J. Moore, N. Vasilieva, J. Sui, S. K. Wong, M. A. Berne, M. Somasundaran, J. L. Sullivan, K. Luzuriaga, T. C. Greenough, H. Choe, M. Farzan, *Nature* **2003**, *426*, 450–454.
- [13] L. Cantuti-Castelvetri, R. Ojha, L. D. Pedro, M. Djannatian, J. Franz, S. Kuivanen, F. van der Meer, K. Kallio, T. Kaya, M. Anastasina, T. Smura, L. Levanov, L. Szirovicza, A. Tobi, H. Kallio-Kokko, P. Osterlund, M. Joensuu, F. A. Meunier, S. J. Butcher, M. S. Winkler, B. Mollenhauer, A. Helenius, O. Gokce, T. Tessalu, J. Hepojoki, O. Vapalahti, C. Stadelmann, G. Balistreri, M. Simons, *Science* **2020**, *370*, 856–860.
- [14] P. Wang, M. S. Nair, L. Liu, S. Iketani, Y. Luo, Y. Guo, M. Wang, J. Yu, B. Zhang, P. D. Kwong, B. S. Graham, J. R. Mascola, J. Y. Chang, M. T. Yin, M. Sobieszczyk, C. A. Kyratsous, L. Shapiro, Z. Sheng, Y. Huang, D. D. Ho, *Nature* **2021**, *593*, 130–135.
- [15] P. Wang, R. G. Casner, M. S. Nair, M. Wang, J. Yu, G. Cerutti, L. Liu, P. D. Kwong, Y. Huang, L. Shapiro, D. D. Ho, *Cell Host Microbe* **2021**, *29*, 747–751.
- [16] F. Grabowski, G. Preibisch, S. Gizniski, M. Kochanczyk, T. Lipniacki, *Viruses* **2021**, *13*, 392.
- [17] Y. Liu, J. Liu, K. S. Plante, J. A. Plante, X. Xie, X. Zhang, Z. Ku, Z. An, D. Scharton, C. Schindewolf, V. D. Menachery, P.-Y. Shi, S. C. Weaver, *BioRxiv* **2021**, <https://doi.org/10.1101/2021.03.08.434499>.
- [18] B. Luan, H. Wang, T. Huynh, *FEBS Lett.* **2021**, *595*, 1454–1461.
- [19] F. Ali, A. Kasry, M. Amin, *Med. Drug Discovery* **2021**, *10*, 100086.
- [20] E. Socher, M. Conrad, L. Heger, F. Paulsen, H. Sticht, F. Zunke, P. Arnold, *BioRxiv* **2021**, <https://doi.org/10.1101/2021.04.06.438584>.
- [21] Q. Li, J. Nie, J. Wu, L. Zhang, R. Ding, H. Wang, Y. Zhang, T. Li, S. Liu, M. Zhang, C. Zhao, H. Liu, L. Nie, H. Qin, M. Wang, Q. Lu, X. Li, J. Liu, H. Liang, Y. Shi, Y. Shen, L. Xie, L. Zhang, X. Qu, W. Xu, W. Huang, Y. Wang, *Cell* **2021**, *184*, 2362–2371.e9.
- [22] S. Dallakyan, A. J. Olson, *Chem. Biol.* **2014**, *243*–250.
- [23] O. Trott, A. J. Olson, *J. Comput. Chem.* **2010**, *31*, 455–461.
- [24] N. Grodsky, Y. Li, D. Bouzida, R. Love, J. Jensen, B. Nodes, J. Nonomiya, S. Grant, *Biochemistry* **2006**, *45*, 13970–13981.
- [25] M. S. Donia, M. A. Fisehbach, *Science* **2015**, *349*, 1254766.
- [26] J. R. Brestoff, D. Artis, *Nat. Immunol.* **2013**, *14*, 676–684.
- [27] A. Agus, K. Clement, H. Sokol, *Gut* **2020**, *70*, 1174–1182.
- [28] V. Kumar, S. Kancharla, M. K. Jena, *VirusDisease* **2021**, *32*, 1–9.
- [29] J. Acosta-Elias, R. Espinosa-Tanguma, *Front. Pharmacol.* **2020**, *11*, 1062.
- [30] A. Dehghani-Samani, M. Kamali, F. Hoseinzadeh-Chahkandak, *Mod. Care J.* **2020**, *17*, e104740.
- [31] S. V. Giofre, E. Napoli, N. Iraci, A. Speciale, F. Cimino, C. Muscara, M. S. Molonia, G. Ruberto, A. Saija, *Comput. Biol. Med.* **2021**, *134*, 104538.
- [32] N. Behloul, S. Baha, Y. Guo, Z. Yang, R. Shi, J. Meng, *Eur. J. Pharmacol.* **2021**, *890*, 173701.
- [33] A. Carino, F. Moraca, B. Fiorillo, S. Marchiano, V. Sepe, M. Biagioli, C. Finamore, S. Bozza, D. Francisci, E. Distrutti, B. Catalanotti, A. Zapella, S. Fiorucci, *Front. Chem.* **2020**, *8*, 572885.
- [34] Q. M. Hanson, K. M. Wilson, M. Shen, Z. Itkin, R. T. Eastman, P. Shinn, M. D. Hall, *ACS Pharmacol. Transl. Sci.* **2020**, *3*, 1352–1360.
- [35] Y. Watanabe, J. D. Allen, D. Wrapp, J. S. McLellan, M. Crispin, *Science* **2020**, *369*, 330–333.
- [36] E. P. Barros, L. Casalino, Z. Gaieb, A. C. Dommer, Y. Wang, L. Fallon, L. Raguetto, K. Belfon, C. Simmerling, R. E. Amaro, *Biophys. J.* **2021**, *120*, 1072–1084.
- [37] T. Sztain, S.-H. Ahn, A. T. Bogetti, L. Casalino, J. A. Goldsmith, R. S. McCool, F. L. Kearns, J. A. McCammon, J. S. McLellan, L. T. Chong, R. E. Amaro, *bioRxiv* **2021**, <https://doi.org/10.1101/2021.02.15.431212>.
- [38] A. Khan, D.-Q. Wei, K. Kousar, J. Abubaker, S. Ahmad, J. Ali, F. Al-Mulla, S. S. Ali, N. Nizam-Uddin, A. Mohammad Sayaf, A. Mohammad, *ChemBioChem* **2021**, <https://doi.org/10.1002/cbic.202100191>.
- [39] L. P. Schenck, M. G. Surette, D. M. Bowdish, *FEBS Lett* **2016**, *590*, 3705–3720.
- [40] C. Kumpitsch, K. Koskinen, V. Schopf, C. Moissl-Eichinger, *BMC Biol* **2019**, *17*, 87.

---

Manuscript received: July 14, 2021  
Accepted manuscript online: July 15, 2021  
Version of record online: July 26, 2021